

# Effects of the polymer molecular weight and type of cation on phase diagrams of polyethylene glycol + sulfate salts aqueous two-phase systems

Gholamhossein Parmoon<sup>1</sup>, Abdorreza Mohammadi Nafchi<sup>2,1</sup> and Mohsen Pirdashti<sup>3</sup>

<sup>1</sup>Department of Chemical Engineering, Damghan Branch, Islamic Azad University, Damghan, Iran

<sup>2</sup>School of Industrial Technology, Universiti Sains Malaysia, 11800, Penang, Malaysia

<sup>3</sup>Faculty of Chemical Engineering, Shomal University, Amol, Iran

## Abstract

Phase diagrams and liquid – liquid equilibrium (LLE) data for aqueous two-phase systems (ATPSs) containing zinc sulfate, magnesium sulfate or aluminium sulfate and polyethylene glycols PEG 300, 400 and 600 have been determined at 298.15 K. It was attempted to show how the PEG molecular weight and the type of cation influence the binodal curve, tie line length (TLL) and slope of the tie line (STL). The results have shown that as the PEG molecular weight increases, the two-phase region becomes extended and the binodal curve shifts to the origin. The refractive index and density of ternary (PEG 300,400 and 600 + zinc sulfate/magnesium sulfate/aluminium sulfate + water) systems have been measured to achieve the phase composition and the tie lines. Finally, the effective excluded volume (EEV) model was applied to describe the salting-out ability of the systems. The LLE data from this research may be potentially used for recovering biological molecules like proteins.

**Keywords:** Liquid–liquid equilibrium; salting-out; density

Available on-line at the Journal web address: <http://www.ache.org.rs/HI/>

SCIENTIFIC PAPER

UDK: 66.061.14: 66.065.31:  
675.043.8+ 676.014.82

*Hem. Ind.* **73** (6) 375-385 (2019)

## 1. INTRODUCTION

Aqueous two-phase systems (ATPSs) are used in liquid- liquid extraction that was first introduced by Beijerinck in 1896; then, Albertsson used these systems to recover biological molecules like proteins and cells [1]. Use of ATPSs has been favored as an effective separation method because of simple scale-up [2], economic effectiveness [3], simple operation as a continuous process [4], reduced interfacial tension [5], short processing time [6], low energy consumption [7], good resolution [8], high yield [9], comparatively high load capacity [10], and selective extraction [11]. Thus, applying ATPSs would be useful for various industries including biotechnology, petroleum, paint, adhesives, and pharmaceuticals [12]. Polyethylene glycol (PEG) is a low toxicity, inexpensive, odorless, neutral, hydrophilic and biocompatible polymer that dissolves in water; it has been applied efficiently in ATPSs [13]. Therefore, there are numerous liquid – liquid equilibrium (LLE) data in literature for systems consisting of PEG (of different molecular weights) and a salt such as PEG (2000, 6000, and 10000) + sodium nitrate at 298.15 K [14], PEG 4000 + disodium tartrate at 298.15-318.15 K [15], PEG (600, 1000, 2000, 4000, and 6000) and sodium citrate at pH (6, 7, and 8) [16]. Also in our previous work we have reported LLE data for PEG 3000 + trisodium citrate [17], PEG 1500 + zinc sulfate [18], PEG 3000 + potassium formate [19], PEG 1500 and 6000 + di-potassium tartarate [20], PEG 3000 + tri-potassium citrate [21] and PEG 600, 1500, 3000, 6000 + sodium formate, potassium formate [22]. In literature, only a few LLE experimental data for the system PEG (of lower molecular weights than 1000) + sulfate salts + water is available [23]. PEG and its chemical derivatives of low molecular weights differ significantly from those PEGs of higher molecular weights in their physico-chemical properties, biological effects on cell permeability and their absorption and excretion, as well as their higher

Corresponding author: Abdorreza Mohammadi Nafchi, School of Industrial Technology, Universiti Sains Malaysia, 11800, Penang, Malaysia;  
Fax: +604 653 5207

E-mail: [amohammadi@usm.my](mailto:amohammadi@usm.my)

Paper received: 03 October 2019

Paper accepted: 15 December 2019

<https://doi.org/10.2298/HEMIND191003035P>



toxicity and possibly genotoxicity [24]. One important point of application of these systems is in complexed biopolymers for nanoencapsulation purposes [25-28].

To the best of our knowledge, reports on LLE data for ATPs with PEG 300, 400, and 600 - zinc sulfate, magnesium sulfate or aluminium sulfate do not exist. Consequently, in the current study, phase diagrams for the above ATPs were measured. In addition, effects of the PEG molecular weight and type of cation on the binodal curve, tie-line length (TLL), and slope of the tie line (STL) were investigated. Also, the calibration curves were used as an analytical technique to determine the phase composition and the end of the tie line. Accordingly, the binodal curves were satisfactorily correlated by the Pirdashti equation [22]. Finally, the effective excluded volume (EEV) model was applied to describe the salting-out ability of the systems.

## 2. EXPERIMENTAL

### 2.1. Materials

To prepare the materials, PEG with average molecular weights of 300, 400, and 600 g mol<sup>-1</sup> were obtained from Merck (Darmstadt, Germany) and zinc sulfate, magnesium sulfate, and aluminum sulfate were obtained from Sigma Aldrich (Dorset, UK), all with minimum purities of 99.5 % by mass. These substances were used without further purification. Distilled deionized water (conductivity=17.5  $\mu\text{S cm}^{-1}$ ) was used for preparation of the solutions. The chemical name, CAS number, source, purification method and purity that provided by producer company are shown in Table 1.

Table 1. Pure components used in this work

Chemical name	Source	CAS Number	Initial mole fraction purity	Purification method	Final mole fraction purity
PEG 300	Merck	25322-68-3	0.99	Crystallization	0.999
PEG 400	Merck	25322-68-3	0.99	Crystallization	0.999
PEG 600	Merck	25322-68-3	0.99	Crystallization	0.999
Zinc sulfate	Sigma Aldrich	7446-20-0	0.99	Fractional crystallization	0.9997
Magnesium sulfate	Sigma Aldrich	7487-88-9	0.99	Fractional crystallization	0.9997
Aluminum sulfate	Sigma Aldrich	17927-65-0	0.99	Fractional crystallization	0.9997

### 2.2. Determination of the binodal curve

To achieve the binodal curve, the cloud-point titration method [17] was used. All tools in these experiments were similar to the research of Pirdashti *et al.* [22]; PEG solutions were used to titrate a salt solution with a known concentration (or vice versa); it was stirred gradually until a cloudy solution was reached. The procedure was repeated to reach other binodal points. The mixture composition was determined by using an analytical balance (model GF300, A&D, Japan) with a precision of  $\pm 10^{-4}$  g.

### 2.3. Determination of tie lines

The tie lines were achieved by designing the equilibrium set according to the method explained earlier by Pirdashti *et al.* [17]. To specify the tie lines, suitable amounts of PEG, salts, and water in a 15 mL graduated cylinder at a chosen PEG molecular weight were mixed to have the feed samples (about 10 g). The mixture was stirred for 5 min and then placed in a thermostated bath with a temperature control by a thermostat (Julabo, Germany) with an accuracy of  $\pm 0.05$  K. Then, to ascertain that the equilibrium is reached and separated into two clear phases, the samples were left to settle for at least 2 h. A centrifuge (HERMLE Labortechnik GmbH Z 206 A, Germany) was used to centrifuge the tubes at 6000 rpm for 5 min to separate the resulting phases; no turbidity was observed, and the top and bottom samples were separated easily. Finally, the concentration of PEG and salt was specified by measuring the density and refractive indices in the top and bottom phases.

The TLL was determined based on experimental measurements of the compositions of the two phases by using the following equation:

$$\text{TTL} = \sqrt{(w_p^{\text{top}} - w_p^{\text{bot}})^2 + (w_s^{\text{bot}} - w_s^{\text{top}})^2} \quad (1)$$

Where  $w_p$  and  $w_s$  indicate the mass fraction of PEG and salt, respectively. The top and bottom phases are designated by superscripts “top” and “bot”, respectively. The ratio of the difference between the concentrations of the polymer and salt in the top and bottom phases allowed the STL calculation by the equation:

$$\text{STL} = \frac{w_p^{\text{top}} - w_p^{\text{bot}}}{w_s^{\text{top}} - w_s^{\text{bot}}} \quad (2)$$

## 2. 4. Binodal curve and TLL correlation

The present system may be useful for commercial applications when considering PEG and salt relationship at the binodal curve. The binodal curves were fitted to the Pirdashti equation [22]:

$$w_p = (a + bw_s)^{-1/c} \quad (3)$$

Here,  $a$ ,  $b$ , and  $c$  are the fitting parameters while  $w_p$  and  $w_s$  are the polymer and salt mass fractions, respectively. Next, the resulting binodal data were correlated by using least-squares regression.

As specified by Guan *et al.* [39], it is possible to determine the salting-out strength of the salt by the effective excluded volume (EEV). Also, the EEV should match the average size of PEG molecules and thus match the weight-average molecular weight of the polymer. It was shown that the larger the molecular weight of the either phase-forming polymer larger is the EEV. Phase formation in the ATPSs is greatly affected by the EEV. Thus, it would be practically useful to establish the link between the EEV and solute volumetric properties since the latter can be easily measured and the former determines the coexistence curve in two-phase systems.

The binodal equation for the aqueous polymer-salt systems can be defined by the following equation [39]:

$$\ln\left(\frac{V^* w_p}{M_p}\right) + \left(\frac{V^* w_s}{M_s}\right) = 0 \quad (4)$$

where  $M_p$  and  $M_s$  represent the molecular weights of the polymer and salt, respectively. Also,  $w_p$  and  $w_s$  are the mass fractions of two phase-forming species along the binodal respectively.  $V^*$  stands for the EEV of the polymer in the aqueous solution of the salt [39].

## 2. 5. Analytical methods

According to our previous work [19], refractive index ( $n_D$ ) and density ( $\rho$ ) of binary (PEG + water, salt + water) and ternary (PEG + salt + water) systems at 298.15 K were measured to determine the compositions in both phases (Supplementary Table S1). A refractometer (QUARTZ RS-232, Ceti, Belgium) with an accuracy of 0.0001  $n_D$  and an Anton Paar oscillation U-tube densitometer (model: DMA 500, Graz, Austria) with a precision of  $\pm 10^{-4}$  g cm<sup>-3</sup> were used to measure the refractive index and density, respectively. Eq. (5) was used to calculate the refractive index and density as a function of salt and PEG concentrations at 298.15 K.

$$Z = a_0 + a_1 w_s + a_2 w_p \quad (5)$$

In eq. (5),  $Z$  stands for the physical property (density or refractive index),  $w_p$  and  $w_s$  stand for the mass fraction of PEG and salt, respectively, and the fitting parameters are shown by  $a_0$ ,  $a_1$ , and  $a_2$ .

## 2. 6. Statistical Analysis

All data were measured twice, and the mean values were reported. The practical data then were fitted to the respected equations by least-squares regression using solver add-in extension implemented to Microsoft Excel 365 TM (Microsoft, USA).



### 3. RESULTS AND DISCUSSION

#### 3.1. Binodal curve

The binodal curve data of the systems PEG 300, 400 and 600 + zinc sulfate/magnesium sulfate/aluminum sulfate + water at 298.15 K are presented in Tables 2 - 4.

Tables 2-4 display the compositions of the phases involved as the PEG molecular weight was varied at 298.15 K. Also, the effects of the molecular weight are shown in Figure 1 and Supplementary Figures S1 and S2. It was observed that increased molecular weight of PEG resulted in biphasic formation at lower concentrations of the polymer and salt. Larger heterogeneous regions were recorded for the PEG 600–salt than for PEG 300, 400–salt ATPs. This finding was predictable since by increasing the polymer molecular weight, hydrophobicity is increased, and water solubility decreases that results in the polymer salting-out. Increased density resulted in insignificant variances in the binodals. Lower density probably affects the decision to choose certain PEG.

Table 2. Binodal curve data of the systems PEG 300, 400 and 600 + zinc sulfate + water at 298.15 K and 0.1 MPa

PEG 300		PEG 400		PEG 600	
100w <sub>p</sub>	100w <sub>s</sub>	100w <sub>p</sub>	100w <sub>s</sub>	100w <sub>p</sub>	100w <sub>s</sub>
99.30	0.35	97.37	0.22	95.72	0.13
91.81	1.40	75.22	2.55	87.65	0.52
80.08	3.68	67.81	3.98	66.32	1.52
57.12	9.00	59.77	5.21	59.63	2.55
46.52	2.57	53.75	6.60	45.22	5.78
32.87	16.3	43.22	9.88	38.62	7.94
27.82	20.32	33.65	12.45	28.55	9.92
21.00	24.75	28.45	14.56	25.45	11.01
12.88	32.45	21.77	17.12	23.12	12.12
9.49	37.26	15.44	22.44	16.55	14.55
6.78	42.56	10.22	28.21	11.22	19.45
4.61	48.62	7.21	33.22	7.55	24.66
2.93	55.74	4.45	39.22	4.77	29.55
2.18	60.42	3.12	45.87	3.22	37.55
1.54	65.87	2.22	51.87	2.18	43.12
99.3	0.35	97.37	0.22	95.72	0.13
91.81	1.40	75.22	2.55	87.65	0.52

Standard uncertainties:  $u(w_i) = 0.002$ ;  $u(P) = 5$  kPa;  $u(T) = 0.05$  K.

Table 3. Binodal curve data of the systems PEG 300, 400 and 600 + magnesium sulfate + water at 298.15 K and 0.1 MPa

PEG 300		PEG 400		PEG 600	
100w <sub>p</sub>	100w <sub>s</sub>	100w <sub>p</sub>	100w <sub>s</sub>	100w <sub>p</sub>	100w <sub>s</sub>
53.53	0.56	50.06	1.00	48.58	0.99
52.65	1.00	48.57	1.43	44.80	2.15
49.27	2.77	45.71	2.64	38.86	3.22
45.13	4.87	37.02	5.96	37.30	4.21
39.52	8.77	35.32	7.47	27.76	9.55
31.90	14.74	30.95	10.54	20.77	14.42
25.60	20.81	21.16	18.87	17.55	19.12
16.62	30.50	17.13	25.09	9.28	28.73
14.32	35.77	12.89	31.23	7.54	30.86
11.68	41.23	10.35	37.56	6.66	35.62
9.81	45.89	8.79	42.22	4.80	41.25
8.41	50.01	6.27	48.77	3.18	48.32
6.75	55.88	4.59	55.68	2.13	55.22
5.78	60.01	3.32	62.45	1.57	60.45
4.56	66.32	3.12	66.87	1.08	66.88
3.90	70.55	2.75	72.55	0.74	73.55
3.01	77.45	3.01	78.61	0.54	78.88

Standard uncertainties:  $u(w_i) = 0.002$ ;  $u(P) = 5$  kPa;  $u(T) = 0.05$  K.

Table 4. Binodal curve data of the systems PEG 300, 400 and 600 + aluminum sulfate + water at 298.15 K and 0.1 MPa.

PEG 300		PEG 400		PEG 600	
100w <sub>p</sub>	100w <sub>s</sub>	100w <sub>p</sub>	100w <sub>s</sub>	100w <sub>p</sub>	100w <sub>s</sub>
46.45	2.13	50.00	1.01	49.26	0.52
39.77	4.16	47.55	1.22	40.00	1.02
35.27	5.30	40.22	2.11	35.65	2.22
30.12	7.87	31.22	5.23	30.12	3.55
25.66	10.55	27.81	7.55	28.61	4.12
22.88	12.65	22.12	10.82	24.18	7.45
19.98	15.44	20.22	12.55	21.45	9.55
18.44	17.25	17.55	14.77	18.55	11.25
16.12	20.55	14.27	18.55	15.22	13.55
15.19	22.14	11.75	22.12	12.82	16.89
13.91	24.61	10.21	25.66	10.22	19.85
12.96	26.73	9.21	27.55	7.55	25.12
12.13	28.86	7.98	29.46	6.55	26.55
11.58	30.42	6.45	32.11	5.77	28.42
10.59	33.75	5.22	35.55	3.87	32.45

Standard uncertainties:  $u(w_i) = 0.002$ ;  $u(P) = 5$  kPa;  $u(T) = 0.05$  K.

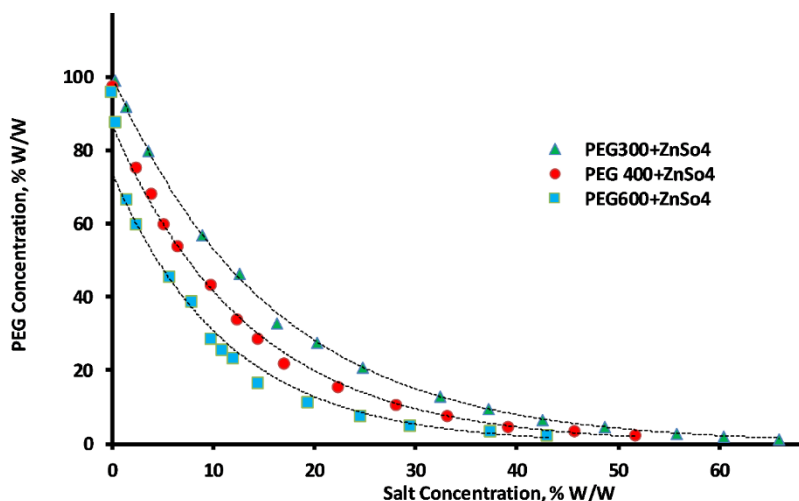


Figure 1. Experimental and correlated binodal curves of PEG 300, 400 and 600 + zinc sulfate + water ATPSS. The dashed lines are calculated from equation (3)

Also Figures 2-4 show the experimental binodal data compared to the data reported in literature [29-33], which show that by using a higher molecular weight polymer, two phase region becomes smaller.

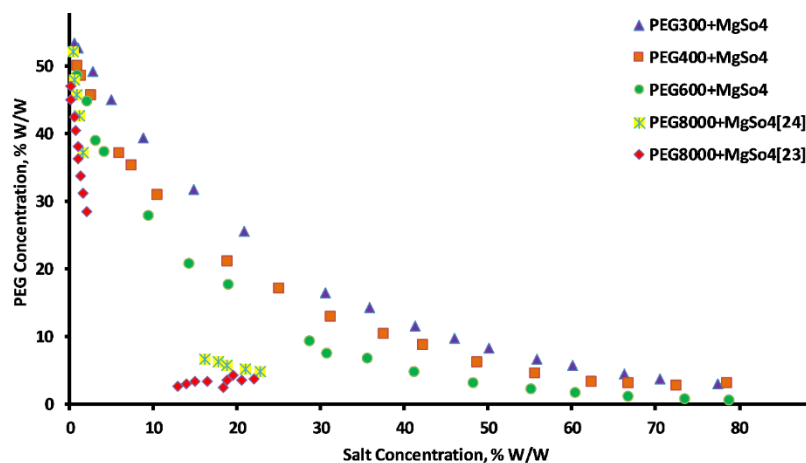


Figure 2. LLE data for systems composed of PEG 300, 400, 600 (present work) and 1500 [24] and 8000 [23] + MgSO<sub>4</sub>

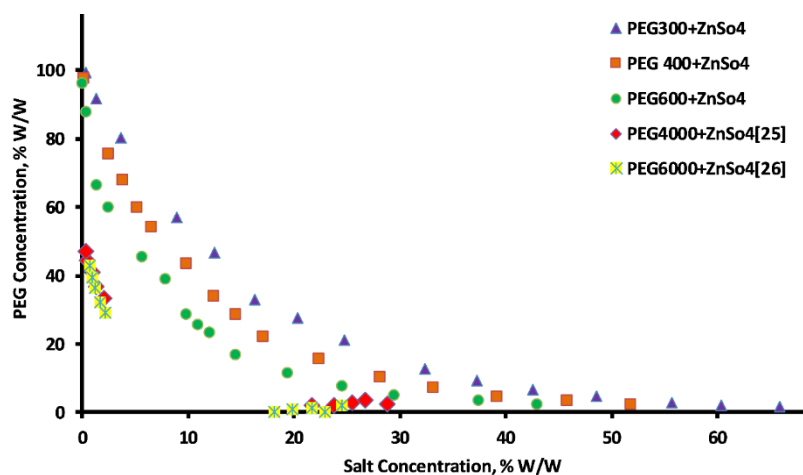


Figure 3. LLE data for systems composed of PEG 300, 400, 600, 4000[25], and 6000[26] +  $ZnSO_4$

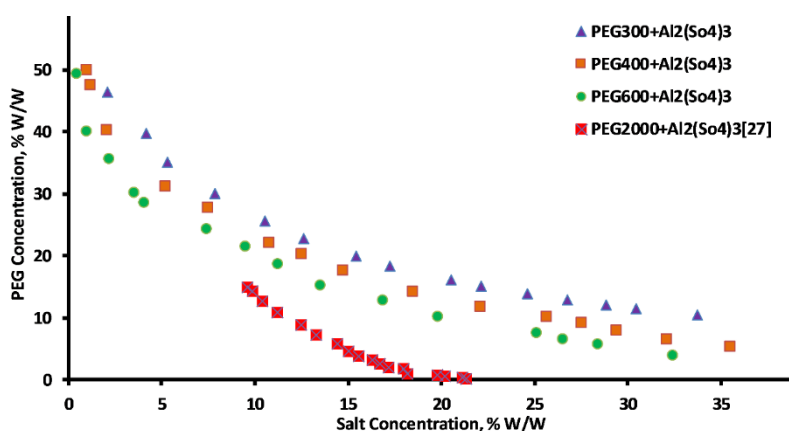


Figure 4. LLE data for systems composed of PEG 300, 400, 600, and 2000 [27] +  $Al_2(SO_4)_3$

### 3. 2. Effects of the salting-out ability of cations on the binodal curve

Figure 5 shows the effects of salting out of the cation (*i.e.* aluminum, magnesium, and zinc cations) in two-phase systems of PEG 300 and sulfate salts. According to the Figure, we find that this effect increases as follows:  $Mg^{2+} < Zn^{2+} < Al^{3+}$ .

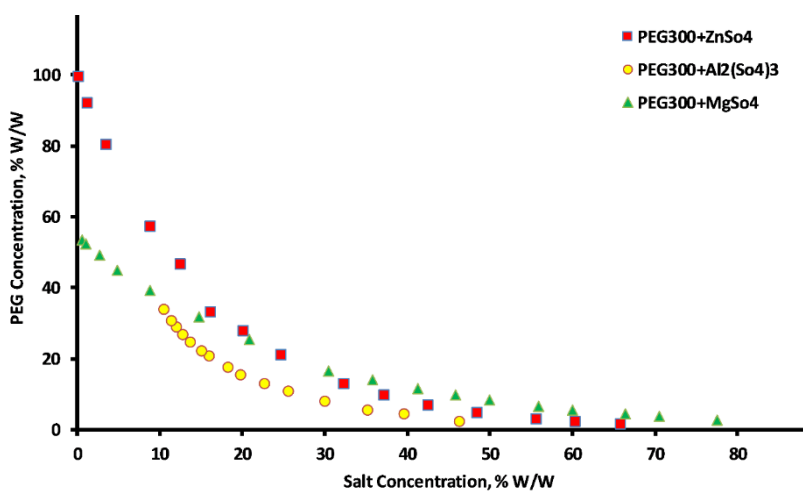


Figure 5. The effect of salting out of the cation in two-phase systems of PEG 300 and sulfate salts

The effect of salting out of cations can be justified based on the Hofmeister series. Cations that have the greatest such effects (exhibiting strong interactions with water molecules) are known as structure-makers or kosmotropes.

### 3. 3. Tie- line data

Table 5 and 6 show how the PEG molecular weight and salting-out of salts influences the equilibrium phase compositions, the slope, and length of the tie lines based on the PEG 300 + zinc sulfate/magnesium sulfate/aluminum sulfate + water systems.

Table 5: Top phase composition, tie-line data and physical properties of PEG 300 + zinc sulfate, Magnesium sulfate and Aluminum sulfate + water aqueous two-phase system at 298.15 K and 0.1 MPa

Salt	Total system		Top phase			
	Mass fraction, %		100w <sub>p</sub>	100w <sub>s</sub>	$\rho (\pm 0.0001) / \text{kg m}^{-3}$	n <sub>D</sub>
	100w <sub>p</sub>	100w <sub>s</sub>				
Magnesium sulfate	31.00	17.00	39.61	8.78	1.1120	1.3924
	32.00	17.00	42.00	7.00	1.1034	1.3953
	33.00	17.00	44.50	6.00	1.1021	1.3905
	34.00	17.00	47.00	4.00	1.0986	1.3982
Zinc sulfate	40.00	15.00	62.00	8.00	1.1040	1.4039
	41.00	15.00	66.00	7.00	1.1041	1.4055
	42.00	15.00	68.00	6.00	1.1037	1.4069
	43.00	15.00	71.00	5.00	1.1033	1.4083
Aluminum sulfate	30.00	15.00	48.00	2.00	1.0653	1.3932
	30.00	16.00	50.00	1.00	1.0697	1.3998
	30.00	17.00	51.00	1.00	1.0731	1.4000
	30.00	18.00	53.00	0.88	1.0753	10.80

As the salt cation is more kosmotropic, the TLL and STL are greater, resulting in a larger two-phase region, and validity of this conclusion is confirmed by these numbers presented in Table 6. The ability of salting out of aluminium cation is higher than those of zinc and magnesium cations, shifting a two-phase curve to the lower part, while the length and slope of the tie line is higher than those of the other cations. Such behavior has been observed in other related work [34,35]. Table 5 shows the tie line compositions for the PEG 300 + sulfate salts ATPSs that were experimentally determined.

Table 6: Bottom phase composition, tie-line data and physical properties of PEG 300 + zinc sulfate, Magnesium sulfate and Aluminum sulfate + water aqueous two-phase system at 298.15 K and 0.1 MPa.

Salt	Total system		Bottom phase				TTL, %	-STL, %
	Mass fraction, %		100w <sub>p</sub>	100w <sub>s</sub>	$\rho (\pm 0.0001) / \text{g m}^{-3}$	n <sub>D</sub>		
	100w <sub>p</sub>	100w <sub>s</sub>						
Magnesium sulfate	31.00	17.00	17.50	30.50	1.2152	1.388	30.99	1.02
	32.00	17.00	16.20	33.00	1.2239	1.388	36.63	0.99
	33.00	17.00	15.88	35.00	1.207	1.396	40.74	0.98
	34.00	17.00	14.25	37.00	1.2596	1.391	46.49	0.97
Zinc sulfate	40.00	15.00	20.00	23.00	1.3998	1.407	41.79	2.60
	41.00	15.00	20.00	25.00	1.3882	1.407	49.40	2.56
	42.00	15.00	19.00	26.00	1.3506	1.407	52.92	2.45
	43.00	15.00	17.00	27.00	1.3522	1.409	58.31	2.35
Aluminum sulfate	30.00	15.00	12.00	29.00	1.2257	1.390	46.00	1.33
	30.00	16.00	12.00	30.00	1.0935	1.397	49.80	1.31
	30.00	17.00	12.00	31.00	1.2675	1.395	52.20	1.30
	30.00	18.00	12.00	32.00	1.3835	4.195	59.47	1.29

Al<sub>2</sub>(SO<sub>4</sub>)<sub>3</sub> proved to be the most effective in ATPS formation, providing the greatest heterogeneous region in the phase diagram (Fig. 6). A thermodynamic approach using the Gibbs free energy of hydration ( $\Delta G_{\text{hyd}}$ ) has been used to

quantify the Hofmeister series and order the salts from kosmotropic to chaotropic. Kosmotropic ions have large negative  $\Delta G_{\text{hyd}}$  due to the resulting structured water lattice around the ion, and therefore the salting-out effect of  $\text{Al}^{3+}$  is greater than those of  $\text{Zn}^{2+}$  and  $\text{Mg}^{2+}$ .

Consistent with previous results, Table 5 shows that the increased kosmotropic power of cations led to the increased slope and length of tie lines [36]. In similar studies [37,38], the cause was attributed to the likely decrease in the thermodynamic volume, and a more compact structure of polymer chains in water. To highlight the involvement of salting-out in the equilibrium phase composition, Figure 6 shows the data of the tie lines, clearly indicating extension of the biphasic region as the kosmotropic power of the cation is increased.

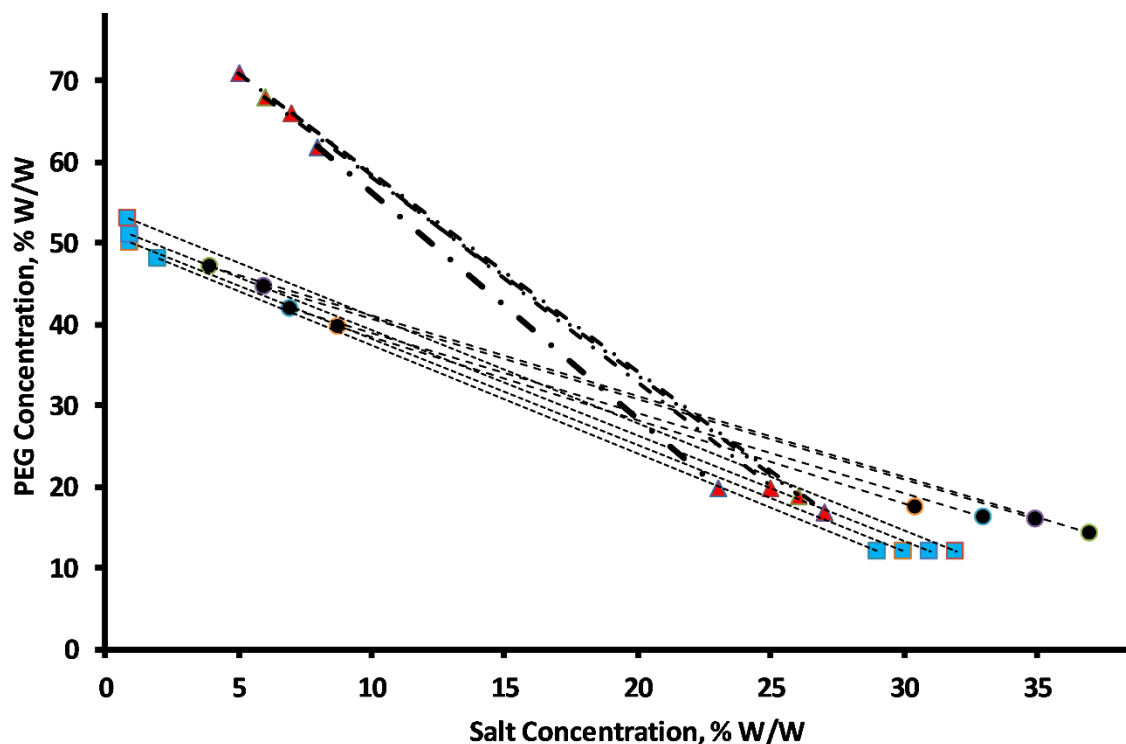


Figure 6. Effects of the cation in sulfate salts on the equilibrium phase composition and slope and length of the tie-line for the PEG 300 + zinc sulfate (▲), PEG 300 + magnesium sulfate (●), PEG 300 + aluminum sulfate (■)

### 3. 4. Binodal curve and tie line data correlation

Table 7 shows the constants in the Pirdashti equation (eq. 3) along with the corresponding  $R^2$  values, determined by the regression analysis of the binodal data for different polymer molecular weights  $R^2$  at 298.15 K.

Table 7. Values of parameters in eq. (3) for the systems PEG + sulfate salt+ water with different PEG molecular weights

PEG molar mass, g mol <sup>-1</sup>	<i>a</i>	<i>b</i>	<i>c</i>	$R^2$
Zinc sulfate				
300	0.9523	0.0006	0.0106	0.9993
400	0.5213	0.0069	0.1421	0.9987
600	0.0513	0.0053	0.7414	0.9882
Magnesium sulfate				
300	0.9995	0.0001	0.0018	0.9997
400	0.5135	0.0044	0.1687	0.9987
600	0.7049	0.0040	0.0892	0.9989
Aluminum sulfate				
300	0.0362	0.0032	0.8185	0.9995
400	0.1258	0.0069	0.5213	0.9934
600	0.1053	0.0078	0.5808	0.9811

The  $R^2$  values ( $>0.98$ ) revealed suitability of the eq. (3) for correlating the binodal curves of the study systems, which is also shown in Figure 1.

As presented in Table 8, our experimental binodal data helped us to obtain the EEV values for the investigated salts by using the eq. (4) and a nonlinear least-squares regression method. The findings showed that the EEV increases and salting-out effects of a cation are related in parallel. This is supported by the strong theoretical background (statistical geometry), which allowed evaluation of the salting-out effects of different salts. Finally, it was shown in literature that both studied equation models (eq. 3 and eq. 4) were successful for association of binodal data from polymer/polymer and polymer/salt ATPSs [39,40]. In other words, for the same salt in the studied systems, the greater the value of the  $V^*$  parameter shows that it would be easier to extract PEG from the salt-rich phase to the PEG -rich phase, and consequently the higher phase-separation ability of the system is expected. This result is consistent with the previous studies, in which the larger  $V^*$  value was associated to the higher salting-out ability [41].

Table 8. Effective excluded volume parameter correlation for the systems PEG 300+ salts

Salt	EEV, mol g <sup>-1</sup>	Least square error
Magnesium sulfate	2400.0	0.0154
Zinc sulfate	2560.1	0.0704
Aluminum sulfate	3547.1	0.8299

#### 4. CONCLUSION

New LLE data and tie line compositions for the systems PEG (300, 400, and 600) + zinc sulfate/magnesium sulfate/aluminum sulfate + water at 298.15 K were determined. Moreover, it was shown how the salting-out of cation influences the phase equilibrium data for the systems PEG 300 + zinc sulfate/magnesium sulfate/aluminum sulfate + water. A direct relationship was found between two-phase area expansion and the increase in the PEG molecular weight, which is likely caused by the salting-out effect. The improved salting-out ability of cations led to the increase in the STL and TLL values. It could be concluded that changes were observed in the STL due to the water movement from the top to the bottom phase. Additionally, the results showed that EEV values of aluminum sulfate > zinc sulfate > magnesium sulfate. The results are potentially useful in biological systems and the additional research is recommended for applications of the LLE data for recovering biological materials.

#### REFERENCES

- [1] Albertsson PA. *Partitioning of Cell Particles and Macromolecules*, 3<sup>rd</sup> ed., New York, NY: Wiley-Interscience; 1986.
- [2] Rocha MV, Nerli BB. Molecular features determining different partitioning patterns of papain and bromelain in aqueous two-phase systems. *Int. J. Biol. Macromol.* 2013; 61: 204-211.
- [3] osa P, Azevedo A, Sommerfeld S, Bäcker W, Aires-Barros M. Aqueous two-phase extraction as a platform in the biomanufacturing industry: economical and environmental sustainability. *Biotechnol. Adv.* 2011; 29:559-567.
- [4] Lei X, Diamond AD, Hsu JT, Equilibrium phase behavior of the poly (ethylene glycol)/potassium phosphate/water two-phase system at 4°C. *J. Chem. Eng. Data.* 1990; 35: 420-423.
- [5] Peng Q, Li Z, Li Y. Experiments, correlation and prediction of protein partition coefficient in aqueous two-phase systems containing PEG and K<sub>2</sub>HPO<sub>4</sub> KH<sub>2</sub>PO<sub>4</sub>. *Fluid Phase Equilib.* 1995;107: 303-315.
- [6] Hu R, Feng X, Chen P, Fu M, Chen H, Guo L, Liu B F. Rapid highly efficient extraction and purification of membrane proteins using a microfluidic continuous-flow based aqueous two-phase system. *J. Chromatogr.* 2011; 1218:171-177.
- [7] Naganagouda K, Mulimani V. Aqueous two-phase extraction (ATPE): an attractive and economically viable technology for downstream processing of *Aspergillus oryzae*  $\alpha$ -galactosidase. *Process. Biochem.* 2008; 43: 1293-1299.
- [8] Bradoo S, Saxena R, Gupta R. Partitioning and resolution of mixture of two lipases from *Bacillus stearothermophilus* SB-1 in aqueous two-phase system. *Process. Biochem.* 35; 1-2: 57-62.
- [9] Rito-Palomares M. Practical application of aqueous two-phase partition to process development for the recovery of biological products. *J. Chromatogr. B.* 2004; 807: 3-1.
- [10] Asenjo JA, Andrews BA. Aqueous two-phase systems for protein separation: phase separation and applications, *J. Chromatogr. A.* 2012; 1238: 1-10.
- [11] Rodrigues GD, de Lemos LR, da Silva LHM, da Silva MCH. Application of hydrophobic extractant in aqueous two-phase systems for selective extraction of cobalt. *J. Chromatogr. A.* 1279; 2013: 13-19.



- [12] Zaslavsky BY. *Aqueous two-phase partitioning: physical chemistry and bioanalytical applications*. CRC Press; 1994.
- [13] Großmann C, Tintinger R, Zhu J, Maurer G. Partitioning of low molecular combination peptides in aqueous two-phase systems of poly (ethylene glycol) and dextran in the presence of small amounts of  $K_2HPO_4/KH_2PO_4$  buffer at 293K: Experimental results and predictions. *Biotechnol. Bioeng.* 1998; 60: 699-711.
- [14] Graber T A, Taboada M E, Asenjo J A, Andrews B A, Influence of molecular weight of the polymer on the liquid– liquid equilibrium of the poly (ethylene glycol)+  $NaNO_3 + H_2O$  system at 298.15 K. *J. Chem. Eng. Data.* 2001; 46:765-768.
- [15] Zafarani-Moattar M T, Hamzehzadeh S, Hosseinzadeh S. Phase diagrams for liquid–liquid equilibrium of ternary poly (ethylene glycol)+ di-sodium tartrate aqueous system and vapor–liquid equilibrium of constituting binary aqueous systems at  $T=(298.15, 308.15, \text{ and } 318.15) \text{ K}$ : Experiment and correlation. *Fluid Phase Equilib.* 2008; 268:142-152.
- [16] Raja S, Ramachandra Murty V. Liquid-liquid equilibria of aqueous two-phase systems containing PEG + sodium citrate+ water at various pH. *J. Chem. Sci. Technol.* 2013; 2:169-174.
- [17] Pirdashti M, Movagharnejad K, Rostami AA, Bakhshi H, Mobalegholeslam P. Liquid-liquid Equilibria, Electrical Conductivity, and Refractive Indices of Poly(ethylene glycol) + Sodium Sulfate + Guanidine Hydrochloride Aqueous Two-Phase Systems: Correlation and Thermodynamic Modeling. *Fluid Phase Equilib.* 2016; 417: 29-40.
- [18] Shahrokhi B, Pirdashti M, Mobalegholeslam P, Rostami AA. liquid-liquid equilibrium and physical properties of aqueous mixtures of poly (ethylene glycol) with zinc sulfate at different pH: experiment, correlation and thermodynamic modeling. *J. Chem. Eng. Data.* 2017; 62:1106-1118.
- [19] Ahmadi F, Pirdashti M, Rostami AA. Density, refractive index and liquid-liquid equilibrium data of poly ethylene glycol 3000 + potassium formate + water at different pH values. *Chin. J. Chem. Eng.* 2018; 26:168-174.
- [20] Barani A, Pirdashti M, Rostami AA. Liquid-Liquid equilibrium of poly (ethylene glycol) 1500 + di-potassium tartrate +water at different pH (6.41, 7.74 and 9.05). *Fluid Phase Equilib.* 2018; 459: 1-9.
- [21] Ketabi M, Pirdashti M, Mobalegholeslam P. Liquid-liquid equilibrium and physical properties of aqueous mixtures of poly (ethylene glycol) 3000 with tri-potassium citrate at different pH: experiment, correlation and thermodynamic modeling. *J. Korean Chem. Soc.* 2019; 63:12-23.
- [22] Pirdashti M, Bozorgzadeh A, Ketabi M, Khoiroh I. Phase equilibria of aqueous mixtures of PEG with formate salt: Effects of pH, type of cation, polymer molecular weight and temperature. *Fluid Phase Equilib.* 2019; 485: 158-167.
- [23] Biondi O, Motta S, Mosesso P, Low molecular weight polyethylene glycol induces chromosome aberrations in Chinese hamster cells cultured *in vitro*, Mutagenesis. 2002; 17:261-64.
- [24] Parmoon, G, Mohammadi Nafchi, A, Pirdashti, M, Density, Viscosity, Refractive Index and Excess Properties of Binary and Ternary Solutions of Poly (Ethylene Glycol), Sulfate Salts and Water at 298.15 K. *Phys. Chem. Res.* 2019 7:859-84.
- [25] Rajabi H, Jafari S M, Rajabzadeh G, Sarfarazi M, Sedaghati S, Chitosan-gum Arabic complex nanocarriers for encapsulation of saffron bioactive components. *Colloids Surf., A.* 2019; 578: p.123644.
- [26] Oladzadabbasabadi N, Ebadi S, Nafchi AM, Karim AA, Kiahosseini S R, Functional properties of dually modified sago starch/k-carrageenan films: An alternative to gelatin in pharmaceutical capsules. *Carbohydr. Polym.* 2017; 160:43-51.
- [27] Ghasemi S, Jafari SM, Assadpour E, Khomeiri M. Production of pectin-whey protein nano-complexes as carriers of orange peel oil. *Carbohydr. Polym.* 2017; 177:369-77.
- [28] Akbariazam M, Ahmadi M, Javadian N, Nafchi AM, Fabrication and characterization of soluble soybean polysaccharide and nanorod-rich ZnO bionanocomposite. *Int. J. Biol. Macromol.* 2016; 89:369-75.
- [29] Cunha E V, Aznar M, Liquid– liquid equilibrium in aqueous two-phase (water+ PEG 8000+ salt): Experimental determination and thermodynamic modeling. *J. Chem. Eng. Data.* 2009; 54: 3242-3246.
- [30] Martins J P, Carvalho C D P, Silva L H M D, Coimbra J S D R, Silva M D C H D, Rodrigues G D, Minim L A, Liquid–liquid equilibria of an aqueous two-phase system containing poly (ethylene) glycol 1500 and sulfate salts at different temperatures. *J. Chem. Eng. Data.* 2007; 53: 238-241.
- [31] de Oliveira R M, Coimbra J S D R, Francisco K R, Minim L A, da Silva L H M, Pereira J A M. Liquid– liquid equilibrium of aqueous two-phase systems containing poly (ethylene) glycol 4000 and zinc sulfate at different temperatures. *J. Chem. Eng. Data.* 2008; 53: 919-922.
- [32] Martins J P, de Oliveira F C, dos Reis Coimbra J S, da Silva L H M, da Silva M D C H, do Nascimento I S B. Equilibrium phase behavior for ternary mixtures of poly (ethylene) glycol 6000+ water+ sulfate salts at different temperatures. *J. Chem. Eng. Data.* 2008; 53:2441-2443.
- [33] Jahani F, Abdollahifar M, Haghazari N. Thermodynamic equilibrium of the polyethylene glycol 2000 and sulphate salts solutions. *J. Chem. Thermodyn.* 2014; 69:125-131.
- [34] Zafarani-Moattar M T, Emamian S, Hamzehzadeh S. Effect of temperature on the phase equilibrium of the aqueous two-phase poly (propylene glycol)+ tripotassium citrate system. *J. Chem. Eng. Data.* 2008; 53:456-461.
- [35] Zhang W, Hu Y, Wang Y, Ha J, Ni L, Wu Y. Liquid–liquid equilibrium of aqueous two-phase systems containing poly (ethylene glycol) of different molecular weights and several ammonium salts at 298.15 K. *Thermochimica Acta.* 2013; 560:47-54.
- [36] Zafarani-Moattar M T, Sadeghi R, Hamidi A A. Liquid–liquid equilibria of an aqueous two-phase system containing polyethylene glycol and sodium citrate: experiment and correlation. *Fluid Phase Equilib.* 2004; 219: 149-155.

- [37] Zhang J, Wang Y, Peng Q. Phase behavior of aqueous two-phase systems of cationic and anionic surfactants and their application to the anine extraction. *Korean J. Chem. Eng.* 2013;30: 1284-1288.
- [38] Kabiri-Badr M, Cabezas H. A thermodynamic model for the phase behavior of salt-polymer aqueous two-phase systems. *Fluid Phase Equilib.* 1996; 115: 39-58.
- [39] Guan Y, Lilley T H, Treffry T E. A new excluded volume theory and its application to the coexistence curves of aqueous polymer two-phase systems. *Macromolecules.* 1993; 26: 3971-3979.
- [40] Gonzalez-Amado M, Rodil E, Arce A, Soto A, Rodriguez O. The effect of temperature on polyethylene glycol (4000 or 8000)–(sodium or ammonium) sulfate Aqueous Two Phase Systems. *Fluid Phase Equilib.* 2016; 428:95-101.
- [41] Silvério S C, Rodríguez O, Teixeira J A, Macedo E A. The effect of salts on the liquid–liquid phase equilibria of PEG 600+ salt aqueous two-phase systems. *J. Chem. Eng. Data.* 2013; 58:3528-3535.

## SAŽETAK

### Utjecaji molrnih masa i vrste katjona na fazne dijagrame vodenih dvofaznih sistema koji sadrže polietilen-glikol i sulfate

Golamhossein Parmoon<sup>1</sup>, Abdorreza Mohammadi Nafchi<sup>2,1</sup> i Mohsen Pirdashti<sup>3</sup>

<sup>1</sup>Department of Chemical Engineering, Damghan Branch, Islamic Azad University, Damghan, Iran

<sup>2</sup>School of Industrial Technology, Universiti Sains Malaysia, 11800, Penang, Malaysia

<sup>3</sup>Faculty of Chemical Engineering, Shomal University, Amol, Iran

(Naučni rad)

U ovom radu određeni su fazni dijagrami i podaci o ravnoteži tečno- tečno (liquid – liquid equilibrium, LLE) za vodene dvofazne sisteme koji sadrže cink-sulfat, magnezijum-sulfat ili aluminijum-sulfat i polietilen-glikole različitih molarnih masa (PEG 300, 400 i 600) na 298,15 K, sa ciljem ispitivanja kako molarna masa PEG i vrsta katjona utiču na binodalnu krivu, dužinu ravnotežnih linija (TLL) i njihov nagib (STL). Rezultati su pokazali da sa porastom molarne mase PEG, dvofazna regija postaje proširena i binodalna kriva se pomera prema izvoru. Indeks refrakcije i gustina trokomponentnih sistema (PEG 300,400 i 600 + cink-sulfat / magnezijum-sulfat / aluminijum-sulfat + voda) su mereni da bi se odredili sastavi faza i ravnotežne linije. Primenjen je model efektivne izdvojene zapremine (EEV) da bi se opisala sposobnost sistema za izolovanje. Podaci LLE iz ovog istraživanja mogu se potencijalno koristiti za izolovanje bioloških molekula poput proteina.

*Ključne reči:* tečno-tečna ravnoteža; precipitaciona kristalizacija; gustina





Supplementary material to

## Effects of the polymer molecular weight and type of cation on phase diagrams of polythylene glycol + sulfate salts aqueous two-phase systems

Golamhossein Parmoon<sup>1</sup>, Abdorreza Mohammadi Nafchi<sup>2,1</sup> and Mohsen Pirdashti<sup>3</sup>

<sup>1</sup>Department of Chemical Engineering, Damghan Branch, Islamic Azad University, Damghan, Iran

<sup>2</sup>School of Industrial Technology, Universiti Sains Malaysia, 11800, Penang, Malaysia

<sup>3</sup>Faculty of Chemical Engineering, Shomal University, Amol, Iran

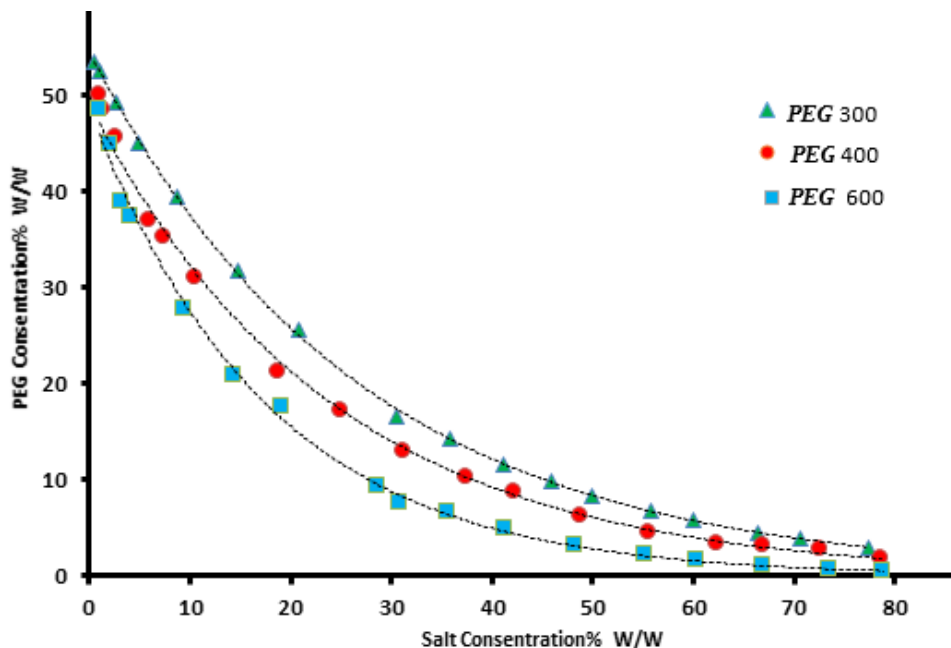


Figure S1. The experimental and correlated binodal curves of PEG 300, 400 and 600 + Magnesium sulfate + water ATPSs. The solid line calculated from equation (3).

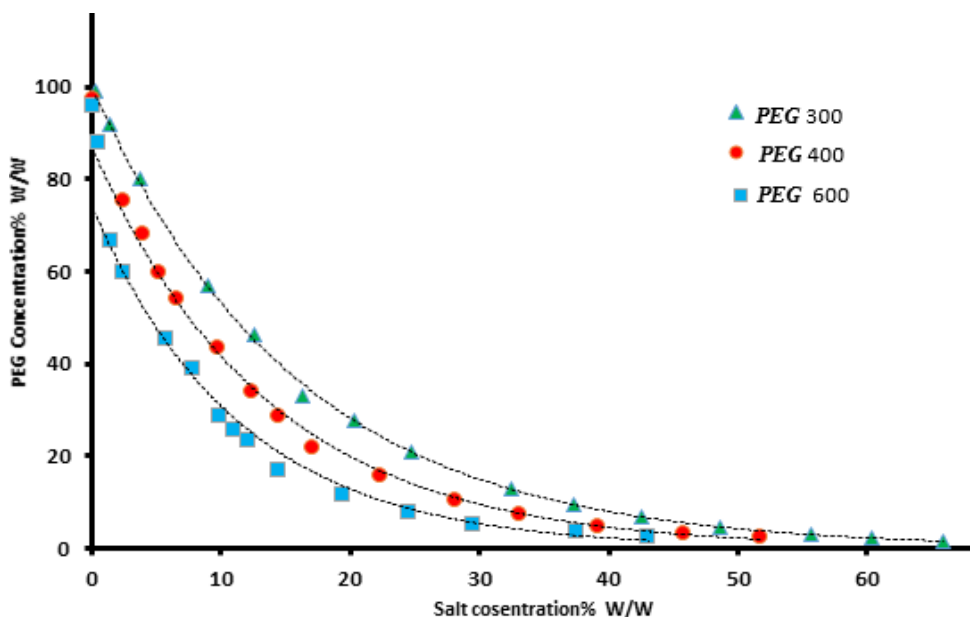


Figure S2. The experimental and correlated binodal curves of PEG 300, 400 and 600 + Aluminum sulfate + water ATPSs. The solid line calculated from equation (3)



**Table S1.** Density,  $\rho$ , and Refractive Index,  $n_D$ , for the binary and ternary of PEG (p) + tri-potassium citrate (s)+ water system at  $298.15 \pm 0.05$  K and  $100 \pm 0.05$  kPa at various mass fractions of polymer,  $w_p$  and salt,  $w_s$ .

$w_p (\pm 0.001) / \% \text{mas}$	$w_s (\pm 0.001) / \% \text{mas}$	$\rho (\pm 0.0001) / \text{kg m}^{-3}$	$n_D (\pm 0.0001)$
PEG 300	Zinc sulfate		
0.05	0.10	1.1899	1.4388
0.10	0.10	1.2885	1.4466
0.15	0.10	1.3588	1.4496
0.20	0.10	1.3855	1.4533
0.25	0.10	1.5577	1.4630
0.00	0.05	1.0255	1.3383
0.00	0.10	1.055	1.3442
0.00	0.15	1.0852	1.3501
0.00	0.20	1.1149	1.3558
0.00	0.25	1.1492	1.3623
0.00	0.30	1.1822	1.3687
0.00	0.00	0.9970	1.3327
0.05	0.00	1.0046	1.3385
0.10	0.00	1.0128	1.3455
0.15	0.00	1.0205	1.3521
0.20	0.00	1.0354	1.3585
0.25	0.00	1.0374	1.3658
0.30	0.00	1.0457	1.3734
1.00	0.00	1.1219	1.4650
PEG 300	Magnesium sulfate		
0.00	0.05	1.0216	1.337
0.00	0.10	1.0473	1.3421
0.00	0.15	1.0728	1.3472
0.00	0.20	1.099	1.3524
0.00	0.25	1.1256	1.3568
0.00	0.30	1.1531	1.3613
0.05	0.15	1.1455	1.3421
0.10	0.15	1.1566	1.3472
0.15	0.15	1.2685	1.3524
0.20	0.15	1.3325	1.3568
0.25	0.10	1.4565	1.3613
PEG 300	Aluminum sulfate		
0.00	0.05	1.0255	1.3383
0.00	0.10	1.055	1.3442
0.00	0.15	1.0852	1.3501
0.00	0.20	1.1149	1.3558
0.00	0.25	1.1492	1.3623
0.00	0.30	1.1822	1.3687
0.05	0.10	1.1899	1.4388
0.10	0.10	1.2885	1.4466
0.15	0.10	1.3588	1.4496
0.20	0.10	1.3855	1.4533
0.25	0.10	1.5577	1.4630

<sup>a</sup>298,15±0.05 K, <sup>b</sup> 100±0.05 kPa